THE JOURNAL OF PHYSICAL CHEMISTRY LETTERS
A JOURNAL OF THE AMERICAN CHEMICAL SOCIETY

pubs.acs.org/JPCL Letter

Binding the Power of Cycloaddition and Cross-Coupling in a Single Mechanism: An Unexpected Bending Journey to Radical Chemistry of Butadiynyl with Conjugated Dienes

Iakov A. Medvedkov,[†] Zhenghai Yang,[†] Anatoliy A. Nikolayev,[†] Shane J. Goettl, André K. Eckhardt, Alexander M. Mebel,* and Ralf I. Kaiser*

Cite This: *J. Phys. Chem. Lett.* 2025, 16, 658−666 Read Online

ACCESS | Metrics & More | Article Recommendations | Supporting Information

ABSTRACT: What if an experiment could combine the power of cycloaddition and cross-coupling with the *in situ* formation of an aromatic molecule in a single collision? Crossed molecular beam experiments augmented with electronic structure and statistical calculations provided compelling evidence on a novel radical route involving 1,3-butadiynyl (HCCCC; $X^2\sum^+$) radicals synthesizing (substituted) arylacetylenes in the gas phase upon reactions with 1,3-butadiene ($CH_2CHCHCH_2$; X^1A_g) and 2-methyl-1,3-butadiene (isoprene; $CH_2C(CH_3)CHCH_2$; X^1A'). This elegant mechanism *de facto* merges two previously disconnected concepts of cross-coupling and cycloaddition−aromatization in a single collision event via the formation of two new $C(sp^2)-C(sp^2)$ bonds and bending the 180° moiety of the linear 1,3-butadiynyl radical out of the ordinary by 60° to 120°. In addition to its importance to fundamental organic chemistry, this unconventional mechanism links two previously separated routes of gas-phase molecular mass growth processes of polyacetylenes and polycyclic aromatic hydrocarbons (PAHs), respectively, in low-temperature environments such as in cold molecular clouds like the Taurus Molecular Cloud (TMC-1) and in hydrocarbon-rich atmospheres of planets and their moons such as Titan, which revises the established understanding of low-temperature molecular mass growth processes in the Universe.

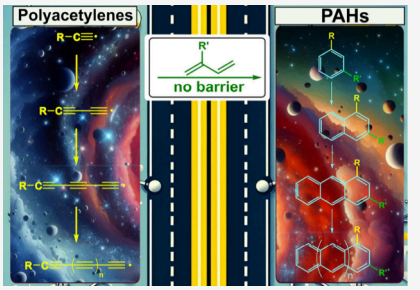

The craft of preparative organic synthesis thrives on two important classes of reactions, the first of which is a classic Diels−Alder[1,2] reaction representing the class of a pericyclic [4 + 2] cycloaddition. In this mechanism, 4π-electrons from an *s-cis* conjugated diene and 2π-electrons from a dienophile (an alkene or alkyne) are involved in the concerted formation of two new carbon−carbon σ-bonds effectively, culminating in a six-membered ring closure process (Scheme 1A). The importance of the Diels−Alder reaction for biochemistry,[3] organic synthetic chemistry,[4,5] materials science,[6] polymers,[7] and the pharmaceutical industry[8] can hardly be overestimated.[9] The second class of reactions that shaped modern synthetic chemistry involves cross-coupling reactions. In this mechanism, two functional groups, such as aryl and alkynyl, are tailored together by a newly formed carbon−carbon bond (Scheme 1B). The iconic Suzuki−Miyaura[10−12] cross-coupling emerged as the second most used reaction in drug-discovery chemistry.[13] The popularity of cross-coupling reactions including Sonogashira[14] and Castro−Stephens[15] is not least explained by the ability to synthesize arylacetylenes − critical π-conjugated systems used as fundamental building blocks for the synthesis of biologically active molecules,[16,17] heterocycles,[18] molecular electronics,[19] and conjugated polymers.[20] However, an "ideal" preparative reaction still remains to be developed, as contemporary pathways are hampered by cyclization reactions excluding aromatization, extensive preparation of the corresponding organohalide precursors, organo-main group reagents, the unavailability of desired synthons, as well as high reaction temperatures.

What if an experiment could combine the power of cycloaddition and cross-coupling with the *in situ* formation of an aromatic molecule in a single collision? Unexpectedly, studying the chemistry of alkynyl radicals opens the door to this "chemical fantasy". Here, we unveil that the linear butadienyl radical (HCCCC; $X^2\sum^+$) participates in an unexpected gas phase cycloaddition−aromatization reaction with conjugated 1,3-butadienes (1,3-butadiene, 2-methyl-1,3-butadiene).

Under single collision conditions, these reactions prepare (substituted) phenylacetylene molecules in the gas phase, thus unconventionally bending the linear butadienyl radical out of the ordinary through incorporation into a 6π Hückel aromatic benzene moiety. The ability of the butadienyl radical to participate in a barrierless aromatization reaction while

Received: November 1, 2024
Revised: November 23, 2024
Accepted: December 2, 2024

https://doi.org/10.1021/acs.jpclett.4c03150
J. Phys. Chem. Lett. 2025, 16, 658−666

Scheme 1. Reaction Schemes for: (A) the Diels–Alder Reaction; (B) Different Cross-Couplings (from Top to Bottom: Suzuki–Miyaura, Sonogashira, and Castro–Stephens); and (C) the Findings of the Current Work[a]

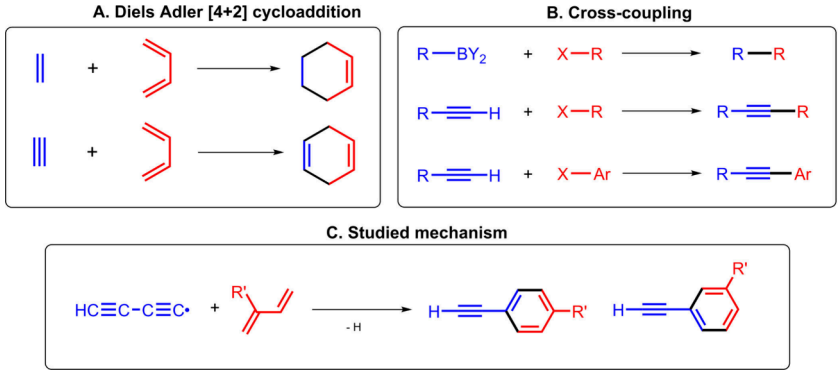

[a]Black bonds–newly formed carbon–carbon bonds.

simultaneously changing the hybridization of two carbon atoms from sp to sp^2 and the linear carbon moiety (180°) to a bent structure (120°) (reactions 1 and 2) challenges classical textbook knowledge of the "expected" reactivity of gas-phase alkynyl radicals as a series of the chain propagations to linear polyacetylenes (reactions 3 and 4).

$$C_4H + CH_2CHCHCH_2 \rightarrow C_6H_5CCH + H \quad (1)$$

$$C_4H + CH_2C(CH_3)CHCH_2 \rightarrow CH_3C_6H_4CCH + H \quad (2)$$

$$HCC + HCCH \rightarrow HCCCCH + H \quad (3)$$

$$HCCCC + HCCH \rightarrow HCCCCCCH + H \quad (4)$$

In this research, we utilized the key strength of gas-phase physical organic chemistry: to study the reaction mechanism with unprecedented detail via crossed molecular beam experiments augmented by high-level quantum chemistry and statistical calculations under single collision conditions. While in the bulk experiments the wall effects and secondary collisions can affect the results, the crossed beam approach has the unique feature of generating the radicals in separate supersonic molecular beams and detecting the output of the reaction after a single collision of reactants. The studied reactions of 1,3-butadiynyl (HCCCC; $X^2\sum^+$) with 1,3-butadiene ($CH_2CHCHCH_2$; X^1A_g) (reaction 1) and of 2-methyl-1,3-butadiene (isoprene; $CH_2C(CH_3)CHCH_2$; X^1A') (reaction 2) represent an elegant and potentially powerful radical mechanism for *de facto* combining cross-coupling and cycloaddition–aromatization in one reaction to synthesize arylacetylenes from acyclic reagents via the construction of two new $C(sp^2)–C(sp^2)$ bonds (Scheme 1C). These data prove a universal and barrierless cycloaddition-aromatization mechanism in reactions of alkynyl radicals with conjugated dienes. Effectively, the conversion of polyacetylenes to aromatic moieties such as benzene in low temperature (10 K) interstellar environments such as in the cold molecular cloud Taurus Molecular Cloud-1 (TMC-1) and in hydrocarbon rich atmospheres of planets and their moons like Titan as well as in high temperature combustion flames of a few 1,000 K links two previously "disconnected" structural concepts (chain extension versus aromatization) and carbon reservoirs (sp versus sp^2). The synthesis of the first aromatic ring in these extreme environments represents a bottleneck process centered on the kinetic models for polycyclic aromatic hydrocarbons (PAHs) formation and growth. Alkynyl radicals are widely present in these environments, and our study unveils a universal, barrierless *initiation* channel for PAHs molecular growth via synthesis of the phenylacetylene structures. In addition, this research introduces an unconventional atom-economical, gas-phase synthesis of arylacetylenes, one of the most common multifunctional synthons in organic synthesis, chemical biology, and material science.

The reactive scattering signal for the reaction of 1,3-butadiynyl (C_4H; 49 amu) with 1,3-butadiene ($CH_2CHCHCH_2$; C_4H_6; 54 amu) was observed at the mass-to-charge ratios of m/z = 102 ($C_8H_6^+$) and 76 ($C_6H_4^+$). The time-of-flight (TOF) spectra obtained at these m/z values overlap after scaling, suggesting that m/z = 76 originates from dissociative electron impact ionization of the C_8H_6 product formed in the 1,3-butadiynyl versus atomic hydrogen exchange pathway (reaction 5). The background signal at m/z = 88 in the primary beam prevented detection of a potential methyl-loss channel (reaction 6); note that the interference signal at m/z = 88 ($C_4H_3{}^{37}Cl^+$) originates from 1,4-dichloro-2-butyne ($C_4H_4Cl_2$) exploited in the synthesis of diacetylene (C_4H_2), i.e. the photolytic precursor of 1,3-butadiynyl (C_4H) (Methods, SI).

For the 1,3-butadiynyl (C_4H; 49 amu) plus 2-methyl-1,3-butadiene ($CH_2C(CH_3)CHCH_2$; 68 amu) reaction, a signal was observed at mass-to-charge ratios of m/z = 116 ($C_9H_8^+$) and 115 ($C_9H_7^+$). The TOFs at m/z = 115 at 116 overlap after scaling, indicating that m/z = 115 originates from dissociative electron impact ionization of the product detected at m/z = 116, with C_9H_8 (116 amu) formed via reaction 7. According to available data from NIST, signals at m/z = 116 and 115 are the two most abundant ion counts for C_9H_8 isomers.[21] No signal was detected at m/z = 102, suggesting an absence of a possible methyl loss channel (reaction 8).

$$C_4H\ (49\ amu) + CH_2CHCHCH_2\ (54\ amu) \rightarrow C_8H_6\ (102\ amu) + H\ (1\ amu) \quad (5)$$

$$C_4H\ (49\ amu) + CH_2CHCHCH_2\ (54\ amu) \rightarrow C_7H_4\ (88\ amu) + CH_3\ (15\ amu) \quad (6)$$

$$C_4H\ (49\ amu) + CH_2C(CH_3)CHCH_2\ (68\ amu) \rightarrow C_9H_8\ (116\ amu) + H\ (1\ amu) \quad (7)$$

https://doi.org/10.1021/acs.jpclett.4c03150
J. Phys. Chem. Lett. 2025, 16, 658–666

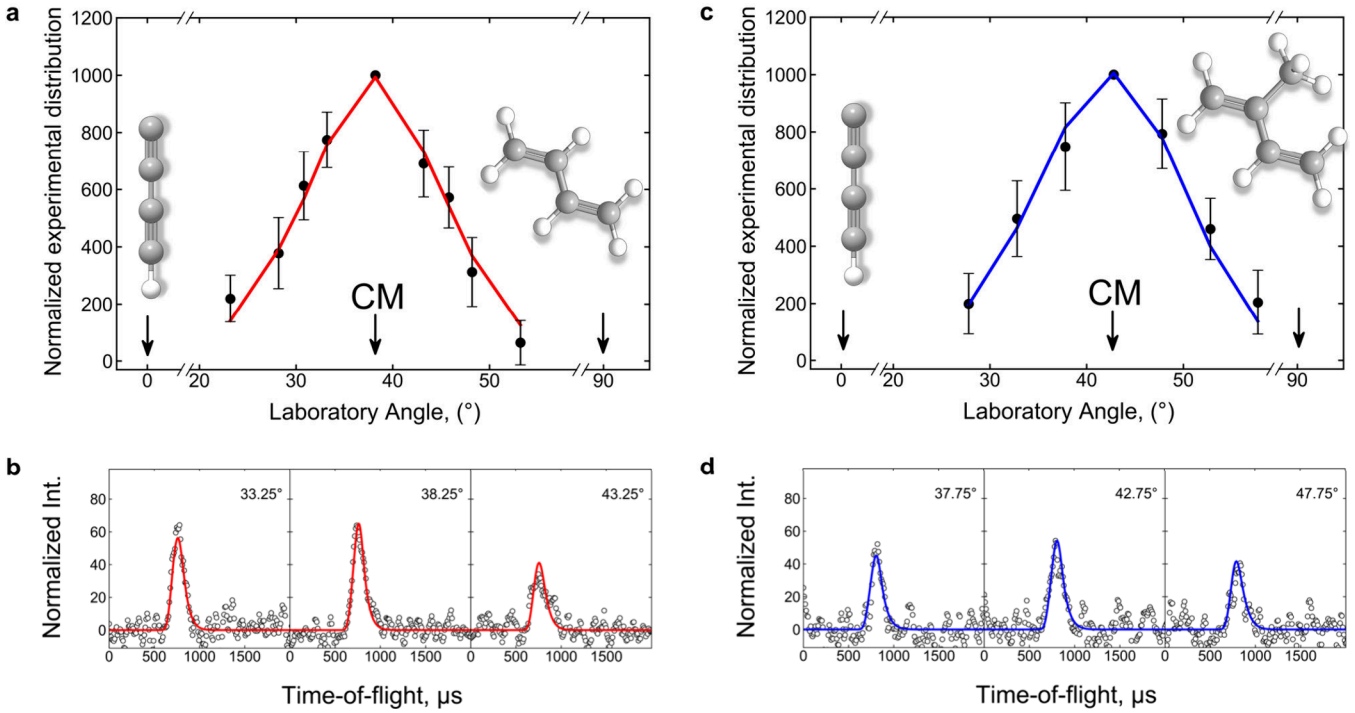

Figure 1. (a) Laboratory angular distribution and (b) time-of-flight (TOF) spectra recorded at m/z = 102 for the reaction of the 1,3-butadiynyl radical with 1,3-butadiene at a collision energy of 22.5 ± 1.0 kJ mol^{-1}. (c) Laboratory angular distribution and (d) time-of-flight (TOF) spectra recorded at m/z = 116 for the reaction of the 1,3-butadiynyl radical with 2-methyl-1,3-butadiene (isoprene) at a collision energy of 23.3 ± 1.2 kJ mol^{-1}. The circles represent the experimental data, and the solid lines are the best fits.

$$C_4H\ (49\ amu) + CH_2C(CH_3)CHCH_2\ (68\ amu) \rightarrow C_8H_6\ (102\ amu) + CH_3\ (15\ amu) \quad (8)$$

The corresponding laboratory angular distributions (LADs) for the reactions of 1,3-butadiynyl with 1,3-butadiene and of 2-methyl-1,3-butadiene systems were recorded at m/z = 102 and 116, respectively (Figure 1a and d). In both systems, the LADs follow the same pattern: they span about 30° of the angular range and depict a forward−backward symmetry with respect to the center-of-mass angle (Θ_{CM}) (Table S1). These findings propose that the reactions of 1,3-butadiynyl with 1,3-butadiene/2-methyl-1,3-butadiene involve indirect reaction dynamics through C_8H_7/C_9H_9 complex(es), which then undergo unimolecular decomposition via atomic hydrogen loss (reactions 5 and 7).

To gain information on the reaction mechanisms, a forward-convolution routine is exploited to convert the laboratory data (TOFs, LADs) into the center-of-mass (CM) reference frame.[22,23] Each system was fitted with a single reaction channel (reaction 5 or 7) with an $E_c^{-2/3}$ dependent reactive cross section at a collision energy E_c; this reflects entrance-barrierless reactions dominated by long-range dipole−dipole interactions.[24]

The resulting best-fit CM functions for both reactions are similar (Figure 2). Let us inspect the center-of-mass translational energy ($P(E_T)$) flux distributions first. Energy conservation dictates that after a reactive collision event, the maximum translational energy (E_{max}) of those products born without internal energy equals the sum of the collisional energy E_C (Table S1) and the reaction energy ($-\Delta_rG$). Here, the $P(E_T)$s for the 1,3-butadiynyl/1,3-butadiene and 1,3-butadiynyl/2-methyl-1,3-butadiene systems hold E_{max} values of 406 ± 29 and 415 ± 22 kJ mol^{-1}, respectively. Therefore, reaction energies were determined to be −383 ± 30 and −392 ± 23 kJ mol^{-1}, respectively, for reactions 5 and 7. Further, both $P(E_T)$s reveal pronounced distribution maxima peaking away from zero translational energy at 30 to 38 kJ mol^{-1}; this finding indicates a tight exit transition state in the exit channel and hence a significant electron reorganization when the reaction intermediate(s) decompose via atomic hydrogen loss to the final products.[24,25] Finally, the average translation energies of 102 ± 7 and 107 ± 6 kJ mol^{-1} suggest that about 26% of the total energy is channeled into product translation; this finding further advocates the formation of covalently bound intermediates and indirect scattering dynamics.[24,26] With respect to the center-of-mass angular distributions, the "best-fit" $T(\theta)$s are isotropic (flat) (Figure 2b and e), as indicative of indirect reactions (complex forming reactions) involving C_8H_7 and C_9H_9 intermediates with life times longer than their rotational periods.[24] The isotropic functions are the direct consequence of the inability of the light hydrogen atom carrying away a significant fraction of the total angular momentum.[24] These findings are also supported by the flux contour maps (Figure 2c and f), which depict an overall image of the reaction and the scattering processes.

In the case of complex, polyatomic systems, it is of advantage to combine our experimental results with electronic structure and statistical calculations to reveal the underlying reaction mechanism and nature of the isomer(s) formed. The computations discovered more than 100 reaction intermediates with the full potential energy surfaces (PES) (Figures S7−S19) along with results of Rice−Ramsperger−Kassel−Marcus (RRKM) calculations (Tables S2−S5) compiled in the Supporting Information. Since these computations (Tables S2 and S3) reveal − supported by our experiments − atomic hydrogen loss channels with branching ratios exceeding 90%

https://doi.org/10.1021/acs.jpclett.4c03150
J. Phys. Chem. Lett. 2025, 16, 658−666

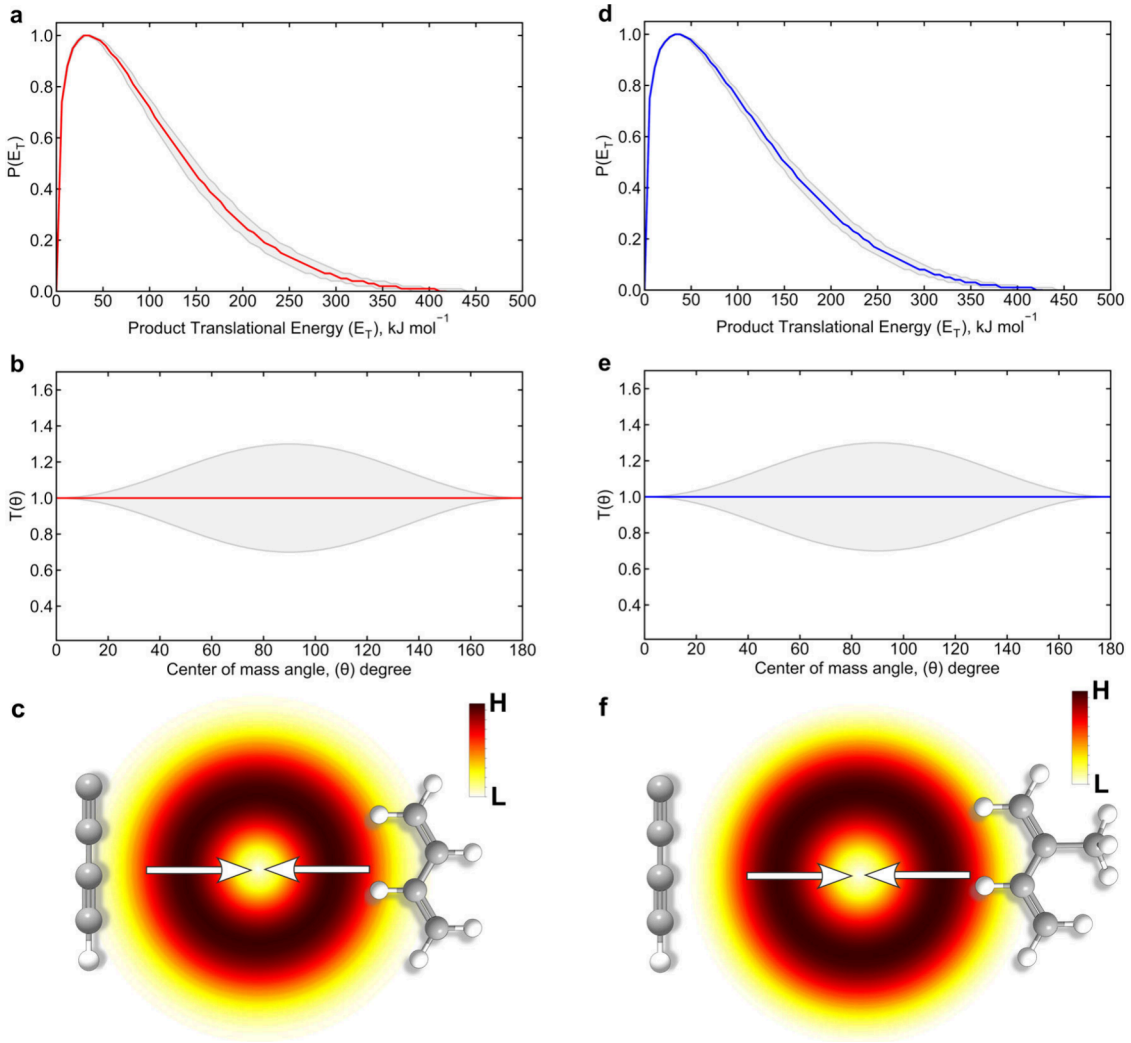

Figure 2. (a) Center-of-mass translational energy ($P(E_T)$), (b) angular distributions ($T(\theta)$), and (c) corresponding flux contour map for the reaction of the 1,3-butadiynyl radical (HCCCC, $X^2\sum^+$) with 1,3-butadiene ($CH_2CHCHCH_2$, X^1A_g). (d) Center-of-mass translational energy, (e) angular distributions, and (f) corresponding flux contour map for the reaction of the 1,3-butadiynyl radical (C_4H, $X^2\sum^+$) with 2-methyl-1,3-butadiene ($CH_2C(CH_3)CHCH_2$, X^1A'). For the $T(\theta)$, the direction of the 1,3-butadiynyl beam is defined as 0° and that of the dienes as 180°. Solid lines represent the best fit, while shaded areas indicate the error limits.

and since discovered mechanisms are similar for 1,3-butadiene and 2-methyl-1,3-butadiene, only H-loss channels for the 1,3-butadiynyl−1,3-butadiene system are discussed in the main manuscript (Figure 3), and the 1,3-butadiynyl−2-methyl-1,3-butadiene system is discussed in detail in SI (Part 3, Figures S11−S12).

For the **1,3-butadiynyl−1,3-butadiene system**, our calculations predict the gas phase preparation of one cyclic (**p1**) and three acyclic (**p4**−**p6**) C_8H_6 product isomers (Figure 3) via atomic hydrogen loss channels. The reaction commences with a barrierless addition of the 1,3-butadiynyl with its radical center to either of the two chemically nonequivalent positions C1 (accessing **i4**) or C2 (accessing **i1**) of the conjugated π electronic system of 1,3-butadiene. Both intermediates can be interconverted rapidly. Intermediate **i1** isomerizes via ring closure through substituted cyclopropanyl radical intermediates **i2** and **i3** followed by ring opening to **i4** and **i6**, respectively. The unimolecular decomposition of **i1** to 3-methyleneocta-1-en-4,6-diyne (**p6**) via hydrogen atom loss is less competitive considering the high energy barrier of 132 kJ mol^{-1} compared to the barrier involved in **i1** → **i2**/**i3** of 44/55 kJ mol^{-1}. Further, the allyl-type resonantly stabilized free radical intermediate **i4** can undergo internal rotation to **i5** followed by a [1,2-H] shift to **i6**; alternatively, **i4** accesses **i6** in a one-step [1,2-H] shift. Both hydrogen shifts **i5** → **i6** and **i4** → **i6** have similar barriers of 160−165 kJ mol^{-1}. Also, **i5** can undergo two additional hydrogen atom migrations. First, a hydrogen shift within the 1,3-butadiene moiety leads to **i8** through a barrier of 129 kJ mol^{-1}; an alternative pathway involves a [1,2-H] shift from the C1 atom of 1,3-butadiene to the 1,3-butadiynyl moiety, accessing **i9** via the barrier of 201 kJ mol^{-1}. Intermediate **i5** can also undergo a facile ring closure, forming a six-membered ring intermediate **i7**; a successive hydrogen migration within the carbon ring forms **i12**. Further, **i8** isomerizes via two competing pathways: a *cis*−*trans* isomerization to **i10** and a hydrogen shift accessing **i9**. Intermediate **i9** holds an *s-cis* diene conformation which allows a low-barrier (24 kJ mol^{-1}) ring closure to **i12**. Alternatively, **i9** can undergo a hydrogen shift to **i11** followed by ring closure to **i13** with low barriers of only 63 and 27 kJ mol^{-1}, respectively. The cyclic intermediate **i12** can interconvert to **i13** via a hydrogen shift. Finally, **i12** and **i13** decompose via hydrogen

https://doi.org/10.1021/acs.jpclett.4c03150
J. Phys. Chem. Lett. 2025, 16, 658−666

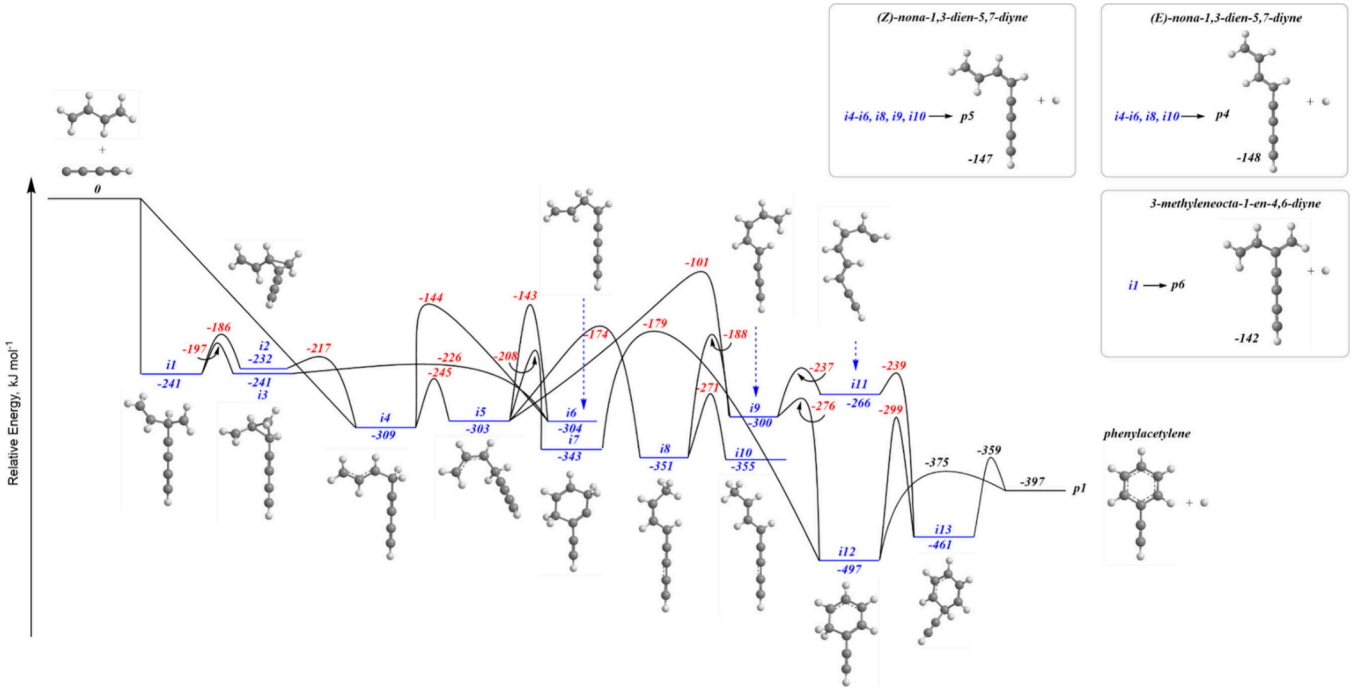

Figure 3. Potential energy surface for the bimolecular reaction of the 1,3-butadiynyl radical (HCCCC, $X^2\sum^+$) with 1,3-butadiene ($CH_2CHCHCH_2$, X^1A_g) leading to C_8H_6 isomers plus the atomic hydrogen calculated at the CCSD(T)-F12/cc-pVTZ-F12//ωB97X-D/6-311G(d,p) level of theory. H-loss exit channels to acyclic products are not shown on the PES but are listed in gray frames.

atom elimination accompanied by aromatization to phenylacetylene (**p1**) in an overall exoergic reaction by −397 kJ mol^{-1}. Alternative atomic hydrogen loss channels are thermodynamically less favorable (Figure 3) with *trans*- and *cis*-nona-1,3-dien-5,7-diyne (**p4** and **p5**) formed from a wide range of intermediates **i4**−**i6**, **i8**, and **i10** → **p4**/**p5** + H and **i9** → **p5** + H, while **p6** can only originate from **i1**.

Which of these pathways dominates the reaction dynamics? A comparison of the experimentally determined reaction energy of −383 ± 30 kJ mol^{-1} with the computed reaction energies suggests that at least the thermodynamically most stable phenylacetylene (**p1**; Δ_rG = −397 ± 5 kJ mol^{-1}) is formed. Less exoergic products **p4**−**p6** might be masked in the lower energy section of the CM translational energy distribution (Figure 2a). According to RRKM calculations (Table S2), **p1** is one of the major reaction products contributing from 23−25% to the total product yield at the experimental collision energy to 37−39% at zero collision energy, with other prevailing products including acyclic **p4** and **p5**. Considering the barriers involved, three pathways involving the central acyclic reaction intermediate **i5** are likely involved in the gas-phase preparation of phenylacetylene (**p1**) (reactions 9−11). The barriers involved suggest that the pathways in reactions 9 and 10 should dominate. This postulation is also confirmed by RRKM calculations (Table S6). Pathways (9) and (10), which include intermediate **i9** with the *s-cis* diene conformation, hold equal branching ratios of 45% and account for more than 90% of **p1** formation. In comparison, pathway (11), where **i5** closes the ring to **i7** in a single step, holds a branching ratio of only 10%.

Overall, the reaction of 1,3-butadiynyl radical with 1,3-butadiene commences with the barrierless addition of the radical center to the conjugated π electronic system of 1,3-butadiene, followed by a series of isomerization steps involving conformational changes via rotations around single C−C bonds, cyclization, and hydrogen shifts prior to hydrogen atom elimination augmented with aromatization to phenylacetylene.

$$\mathbf{i5} \rightarrow \mathbf{i8} \rightarrow \mathbf{i9} \rightarrow \mathbf{i12} \rightarrow \mathbf{p1} + \mathrm{H} \quad (9)$$

$$\mathbf{i5} \rightarrow \mathbf{i8} \rightarrow \mathbf{i9} \rightarrow \mathbf{i11} \rightarrow \mathbf{i13} \rightarrow \mathbf{p1} + \mathrm{H} \quad (10)$$

$$\mathbf{i5} \rightarrow \mathbf{i7} \rightarrow \mathbf{i12} \rightarrow \mathbf{p1} + \mathrm{H} \quad (11)$$

For the **1,3-butadiynyl−2-methyl-1,3-butadiene system**, considering the experimental reaction energy of −392 ± 23 kJ mol^{-1}, the computational results support the gas phase preparation of the aromatic products *m*- and *p*-tolylacetylenes (methylphenylacetylene; **p2** and **p3**; Δ_rG = −391 ± 5 kJ mol^{-1}) plus atomic hydrogen under single collision conditions. These results also align with the statistical calculations, revealing that the formation of both methylphenylacetylene isomers **p2** and **p3** dominates the chemical mechanism with branching ratios of up to 70% (Table S3). The RRKM calculations reveal that the incorporation of the methyl group does not have a significant impact on the overall branching ratios, thus classifying the methyl group as a spectator with branching ratios **p7** and **p8** not exceeding 5%. Three pathways can lead to the aromatic products initiated through radical addition to the C1=C2 (pathways (S1)-(S3)) and C3=C4 (pathways (S4)-(S6)) moieties. Essentially, the RRKM studies support low energy barrier pathways involving *s-cis* diene (**i22** and **i37**) intermediates for more than 97% of all aromatics formed.

Crossed molecular beam experiments augmented with electronic structure and statistical calculations provided compelling evidence on a novel radical route involving 1,3-butadiynyl (HCCCC; $X^2\sum^+$) radicals synthesizing (substituted) arylacetylenes in the gas phase upon reactions with 1,3-butadiene ($CH_2CHCHCH_2$; X^1A_g) and 2-methyl-1,3-butadiene (isoprene; $CH_2C(CH_3)CHCH_2$; X^1A'). This elegant mechanism *de facto* merges two previously disconnected

https://doi.org/10.1021/acs.jpclett.4c03150
J. Phys. Chem. Lett. 2025, 16, 658−666

Scheme 2. A Universal Alkyne−Diene Class of Barrierless Cycloaddition−Aromatization Reactions Can Bridge Two Previously Insulated Mechanisms: Growth of Aromatics and Propagation of Polyacetylenes

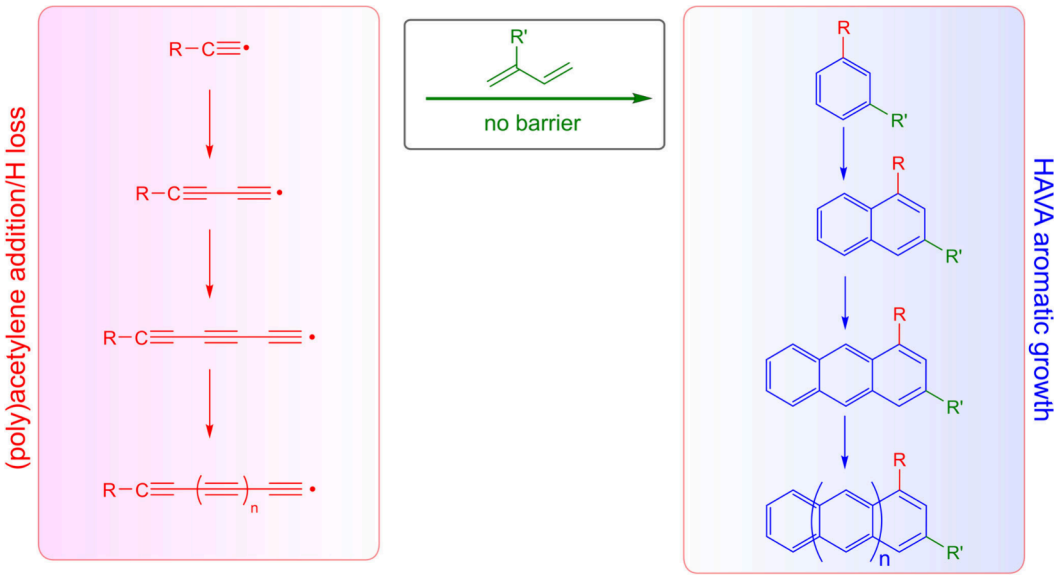

concepts of *cross-coupling* and *cycloaddition−aromatization* in a single collision event via the formation of two new C(sp^2)−C(sp^2) bonds and bending the 180° moiety of the linear 1,3-butadiynyl radical out of the ordinary by 60° to 120° while changing the hybridization of the carbon atoms involved from sp to sp^2. The reaction dynamics are driven by barrierless addition of the 1,3-butadiynyl radical to the diene moiety followed by extensive isomerization series via hydrogen shifts and ring closure predominantly through *s-cis* diene conformers prior to unimolecular decomposition via atomic hydrogen loss accompanied by aromatization in overall exoergic reactions to (substituted) arylacetylenes.

This unconventional cycloaddition−aromatization mechanism links two previously separated routes of gas-phase molecular mass growth processes to polyacetylenes and polycyclic aromatic hydrocarbons (PAHs), respectively, in low-temperature environments such as in cold molecular clouds like the Taurus Molecular Cloud (TMC-1) and in hydrocarbon rich atmospheres of planets and their moons such as Titan (Scheme 2). Polyacetylenes are synthesized via a sequence of simple radical addition−elimination steps of (poly)acetylenyl radicals ($HC{\equiv}C(C{\equiv}C)_n$) with acetylene (m = 0) and lower mass polyacetylenes ($HC{\equiv}C(C{\equiv}C)_mH$) (reaction 12), thus growing linear, hydrogen terminated carbon chains: polyacetylenes.[26−30]

On the other hand, the hydrogen abstraction−vinylacetylene addition mechanism (HAVA) forms aromatic molecules barrierlessly through ring annulation at low temperatures under single collision conditions adding "one ring at a time" (e.g. reactions 13 and 14), leading to naphthalene ($C_{10}H_8$) and anthracene/phenanthrene ($C_{14}H_{10}$), respectively. The newly discovered *cross-coupling* and *cycloaddition−aromatization* mechanism efficiently connects the "polyacetylene/polyacetylenyl" carbon reservoir with the "aromatic" carbon reservoir, thus initiating a complex chain of bimolecular collisions commencing with the reaction of 1,3-butadienyl radicals with 1,3-butadiene and 2-methyl-1,3-butadiene in low temperature environments. Eventually, ethynyl[31−33] and polyacetylenyl radicals, in which the hydrogen atom is substituted by, e.g., methyl or phenyl groups, may form highly substituted aromatic structures in barrierless, exoergic reactions with 1,3-butadiene and 2-methyl-1,3-butadiene regardless of the nature of the substituent in the "polyacetylenyl" radical reactant. It is important to note that in dense hydrocarbon rich atmospheres of planets and their moons such as of Titan, photochemically (144−255 nm) activated triplet diacetylene (C_4H_2*) may react with 1,3-butadiene to phenylacetylene (C_6H_5CCH).[34] However, this mechanism cannot operate in cold molecular clouds due to the relaxation of triplet diacetylene. On the other hand, the novel *cross-coupling* and *cycloaddition−aromatization* mechanism represents a versatile route of aromatization accessing substituted benzenes, thus initiating aromatization and low temperature molecular mass growth processes in our universe.

$$HC{\equiv}C(C{\equiv}C)_n + HC{\equiv}C(C{\equiv}C)_mH \rightarrow HC{\equiv}C(C{\equiv}C)_{(n+m)}H + H \quad (12)$$

$$C_6H_5 + C_4H_4 \rightarrow C_{10}H_8 + H \quad (13)$$

$$C_{10}H_7 + C_4H_4 \rightarrow C_{14}H_{10} + H \quad (14)$$

MATERIALS AND METHODS

Crossed Molecular Beams. The reactions of 1,3-butadiynyl (C_4H; $X^2\Sigma^+$) with 1,3-butadiene ($CH_2CHCHCH_2$; X^1A_g) and 2-methyl-1,3-butadiene ($CH_2C(CH_3)CHCH_2$; X^1A') were conducted under single collision conditions exploiting a crossed molecular beams machine. The foundation of the method, the crossed molecular apparatus, and signal analysis have been described elsewhere.[26,35−37] The crossed beams machine consists of a stainless-steel vacuum chamber (10^{-8} Torr) which encloses two source chambers at a crossing angle of 90° and an ultrahigh-vacuum (10^{-12} Torr), rotatable, differentially pumped quadrupole mass spectrometric (QMS) detector (Figure S1). The 1,3-butadiynyl radicals were generated in the primary source chamber by photodissociation of diacetylene (C_4H_2) seeded at a level of 1% in a 4:1 mixture of helium and argon (He and Ar: 99.9999%, Matheson) at a backing pressure of 1 atm. The 193 nm photolysis wavelength

https://doi.org/10.1021/acs.jpclett.4c03150
J. Phys. Chem. Lett. 2025, 16, 658−666

was employed successfully by Sims et al. in low-temperature kinetic studies utilizing the CRESU apparatus.[38−40] Diacetylene is not commercially available and was synthesized by the one-stage method as reported in SI.[41−43] The output of the ArF excimer laser (193 nm, 50 mJ, 30 Hz, Coherent, CompEx110) was focused (1.5 × 3 mm^2) 2 mm away from the exit of the Proch-Trickl pulsed valve.[44] The supersonic beam containing the 1,3-butadiynyl radicals was then collimated with a 1 mm diameter skimmer before entering the reaction chamber. A four-slot chopper wheel located after the skimmer selected a portion of the 1,3-butadiynyl radical beam with a well-defined peak velocity (v_p) and speed ratio (S). In the secondary source chamber, a pulsed molecular beam of neat 1,3-butadiene (99.6%; Sigma-Aldrich) or 2-methyl-1,3-butadiene (99%; Sigma-Aldrich) was released at backing pressures of 550 and 450 Torr, respectively. Primary and secondary beams v_p and S, corresponding collision energies (E_c), and center-of-mass angles (Θ_{CM}) for the studied reactions are gathered in Table S1. The pulse scheme of the experiment is reported in the SI (Figures S2 and S3).

Computational Methods. Geometry optimization of numerous structures on both C_8H_7 and C_9H_9 potential energy surfaces (PESs) of the butadiynyl radical plus 1,3-butadiene and 2-methyl-1,3-butadiene reactions was carried out at the long-range corrected hybrid density functional (DFT) ωB97X-D level of theory[45] with Pople's split-valence 6-311G(d,p) basis set.[46,47] The same theory was used to compute harmonic vibrational frequencies for each optimized stationary point. The frequencies provide us with zero-point vibrational energy corrections (ZPE) and are utilized in calculations of the energy-dependent rate constants.

Single-point energies for all structures on the C_8H_7 PES were amended by means of the explicitly correlated coupled cluster CCSD(T)-F12 approach[48,49] utilizing the variational method for single and double excitations and the perturbation theory for triple excitations accompanied by Dunning's correlation-consistent cc-pVTZ-f12 basis set.[50] As for C_9H_9 PES, the G3(MP2,CC) model chemistry scheme was applied, as the molecular size makes the CCSD(T)-F12 calculations prohibitively expensive. The G3(MP2,CC) energy consists of the coupled cluster CCSD(T)/6-311G(d,p) energy, which is then enhanced by a basis set correction to the G3Large basis set using the Møller−Plesset second-order perturbation theory.[51−53] The first CCSD(T)-F12/cc-pVTZ-f12//ωB97X-D/6-311G(d,p) + ZPE[ωB97X-D/6-311G(d,p)] theoretical scheme is expected to ensure the accuracy within 4 kJ mol^{-1} or even better,[54] and the second G3(MP2,CC)//ωB97X-D/6-311G(d,p) + ZPE(ωB97X-D/6-311G(d,p)) theoretical approach is known to have the accuracy within 10 kJ mol^{-1} or better.[53] The Gaussian 09[55] and Molpro 2015[56] quantum chemistry software packages were employed for all the electronic structure calculations.

Rice−Ramsperger−Kassel−Marcus (RRKM) statistical theory[57−59] was applied to compute microcanonical, internal energy-dependent rate constants of all unimolecular reaction steps on the C_8H_7 and C_9H_9 PESs after the first recombination of the reactants as a consequence of a single collision of the butadiynyl radical with the 1,3-butadiene and 2-methyl-1,3-butadiene compounds. The statistical calculations assumed the zero-pressure limit, thereby simulating the crossed molecular beam single collision conditions related to a deep space environment. The internal energy of all the isomers on both C_8H_7 and C_9H_9 PESs was equal to the sum of the collision and chemical activation energies, where the last term resulted from a negative of the relative energy for all the isomers relative to the separated butadiynyl radical plus 1,3-butadiene and 2-methyl-1,3-butadiene reactants, respectively. Our in-house code Unimol[60] was used to perform the RRKM calculations. The product branching ratios were subsequently evaluated via the calculated rate constants considering steady-state approximation.[60,61]

■ ASSOCIATED CONTENT

Data Availability Statement

The data that support the findings of this study are available in the article and the Supporting Information. Additional data are available from the corresponding authors upon reasonable request.

Supporting Information

The Supporting Information is available free of charge at https://pubs.acs.org/doi/10.1021/acs.jpclett.4c03150.

Details of the crossed molecular beams experiment; diacetylene synthesis; description of 1,3-butadiynyl + 2-methyl-1,3-butadiene PES; full PESs for 1,3-butadiynyl + 1,3-butadiene and 1,3-butadiynyl + 2-methyl-1,3-butadiene systems; results of RRKM calculations; optimized Cartesian coordinates (Å) and vibrational frequencies (cm^{-1}) for all intermediates, transition states, reactants, and products involved. (PDF)

■ AUTHOR INFORMATION

Corresponding Authors

Alexander M. Mebel − *Department of Chemistry and Biochemistry, Florida International University, Miami, Florida 33199, United States;* orcid.org/0000-0002-7233-3133; Email: mebela@fiu.edu

Ralf I. Kaiser − *Department of Chemistry, University of Hawai'i at Mānoa, Honolulu, Hawaii 96822, United States;* orcid.org/0000-0002-7233-7206; Email: ralfk@hawaii.edu

Authors

Iakov A. Medvedkov − *Department of Chemistry, University of Hawai'i at Mānoa, Honolulu, Hawaii 96822, United States*

Zhenghai Yang − *Department of Chemistry, University of Hawai'i at Mānoa, Honolulu, Hawaii 96822, United States*

Anatoliy A. Nikolayev − *Samara National Research University, Samara 443086, Russia*

Shane J. Goettl − *Department of Chemistry, University of Hawai'i at Mānoa, Honolulu, Hawaii 96822, United States;* orcid.org/0000-0003-1796-5725

André K. Eckhardt − *Lehrstuhl für Organische Chemie II, Ruhr-Universität Bochum, 44801 Bochum, Germany;* orcid.org/0000-0003-1029-9272

Complete contact information is available at: https://pubs.acs.org/10.1021/acs.jpclett.4c03150

Author Contributions

†I.A.M, Z.Y., and A.A.N. contributed equally. All authors have given approval to the final version of the manuscript.

Notes

The authors declare no competing financial interest.

https://doi.org/10.1021/acs.jpclett.4c03150
J. Phys. Chem. Lett. 2025, 16, 658−666

■ ACKNOWLEDGMENTS

The experimental studies at the University of Hawaii were supported by the US Department of Energy, Basic Energy Sciences DE-FG02-03ER15411. The electronic structure and kinetic calculations at the Florida International University were funded by the US Department of Energy, Basic Energy Sciences DE-FG0204ER15570. The chemical synthesis was supported by the Deutsche Forschungsgemeinschaft (DFG, German Research Foundation) under Germany's Excellence Strategy - EXC-2033-390677874 - RESOLV and the Fonds der Chemischen Industrie (Liebig Fellowship to A.K.E.).

■ REFERENCES

(1) Diels, O.; Alder, K. Synthesen in Der Hydroaromatischen Reihe. *Justus Liebigs Annalen der Chemie* **1928**, *460* (1), 98−122.
(2) Norton, J. A. The Diels-Alder Diene Synthesis. *Chem. Rev.* **1942**, *31* (2), 319−523.
(3) Stork, G.; Tamelen, E. E. V.; Friedman, L. J.; Burgstahler, A. W. Cantharidin. A Stereospecific Total Synthesis. *J. Am. Chem. Soc.* **1951**, *73* (9), 4501−4501.
(4) Nicolaou, K. C.; Snyder, S. A.; Montagnon, T.; Vassilikogiannakis, G. The Diels−Alder Reaction in Total Synthesis. *Angew. Chem., Int. Ed.* **2002**, *41* (10), 1668−1698.
(5) Funel, J.-A.; Abele, S. Industrial Applications of the Diels−Alder Reaction. *Angew. Chem., Int. Ed.* **2013**, *52* (14), 3822−3863.
(6) Zydziak, N.; Yameen, B.; Barner-Kowollik, C. Diels−Alder Reactions for Carbon Material Synthesis and Surface Functionalization. *Polym. Chem.* **2013**, *4* (15), 4072−4086.
(7) Briou, B.; Améduri, B.; Boutevin, B. Trends in the Diels−Alder Reaction in Polymer Chemistry. *Chem. Soc. Rev.* **2021**, *50* (19), 11055−11097.
(8) Gates, M.; Tschudi, G. The Synthesis of Morphine. *J. Am. Chem. Soc.* **1956**, *78* (7), 1380−1393.
(9) Fringuelli, F.; Taticchi, A. *The Diels-Alder Reaction: Selected Practical Methods*; John Wiley & Sons, 2002.
(10) Miyaura, N.; Yamada, K.; Suzuki, A. A New Stereospecific Cross-Coupling by the Palladium-Catalyzed Reaction of 1-Alkenylboranes with 1-Alkenyl or 1-Alkynyl Halides. *Tetrahedron Lett.* **1979**, *20* (36), 3437−3440.
(11) Miyaura, N..; Suzuki, A.. Palladium-Catalyzed Cross-Coupling Reactions of Organoboron Compounds. *Chem. Rev.* **1995**, *95* (7), 2457−2483.
(12) Miyaura, N.; Suzuki, A. Stereoselective Synthesis of Arylated (E)-Alkenes by the Reaction of Alk-1-Enylboranes with Aryl Halides in the Presence of Palladium Catalyst. *J. Chem. Soc., Chem. Commun.* **1979**, *19*, 866−867.
(13) Boström, J.; Brown, D. G.; Young, R. J.; Keserü, G. M. Expanding the Medicinal Chemistry Synthetic Toolbox. *Nat. Rev. Drug Discov* **2018**, *17* (10), 709−727.
(14) Sonogashira, K.; Tohda, Y.; Hagihara, N. A Convenient Synthesis of Acetylenes: Catalytic Substitutions of Acetylenic Hydrogen with Bromoalkenes, Iodoarenes and Bromopyridines. *Tetrahedron Lett.* **1975**, *16* (50), 4467−4470.
(15) Stephens, R. D.; Castro, C. E. The Substitution of Aryl Iodides with Cuprous Acetylides. A Synthesis of Tolanes and Heterocyclics1. *J. Org. Chem.* **1963**, *28* (12), 3313−3315.
(16) Mitzel, F.; FitzGerald, S.; Beeby, A.; Faust, R. The Synthesis of Arylalkyne-Substituted Tetrapyrazinoporphyrazines and an Evaluation of Their Potential as Photosensitisers for Photodynamic Therapy. *Eur. J. Org. Chem.* **2004**, *2004* (5), 1136−1142.
(17) Bonne, D.; Dekhane, M.; Zhu, J. Modulating the Reactivity of α-Isocyanoacetates: Multicomponent Synthesis of 5-Methoxyoxazoles and Furopyrrolones. *Angew. Chem., Int. Ed.* **2007**, *46* (14), 2485−2488.
(18) Vasilevsky, S. F.; Stepanov, A. A. Alkyl, Aryl, and Hetaryl Acetylenes: Highly Reactive Multifunctional Compounds (A Review). *Russ J. Gen Chem.* **2023**, *93* (10), 2417−2492.
(19) Silvestri, F.; Marrocchi, A. Acetylene-Based Materials in Organic Photovoltaics. *International Journal of Molecular Sciences* **2010**, *11* (4), 1471−1508.
(20) Lam, J. W. Y.; Tang, B. Z. Functional Polyacetylenes. *Acc. Chem. Res.* **2005**, *38* (9), 745−754.
(21) Linstrom, P. NIST Chemistry WebBook, NIST Standard Reference Database 69, 1997. http://webbook.nist.gov/chemistry/ (accessed 2024-04-22).
(22) Vernon, M. F. Molecular Beam Scattering. Ph.D. Dissertation, University of California, Berkeley, CA, 1983.
(23) Weiss, P. S. Reaction Dynamics of Electronically Excited Alkali Atoms with Simple Molecules. Ph.D. Dissertation, University of California, Berkeley, CA, 1986.
(24) Levine, R. D. *Molecular Reaction Dynamics*; Cambridge University Press: Cambridge, UK, 2005.
(25) Laskin, J.; Lifshitz, C. Kinetic Energy Release Distributions in Mass Spectrometry. *J. Mass Spectrom.* **2001**, *36* (5), 459−478.
(26) Kaiser, R. I. Experimental Investigation on the Formation of Carbon-Bearing Molecules in the Interstellar Medium via Neutral−Neutral Reactions. *Chem. Rev.* **2002**, *102* (5), 1309−1358.
(27) Sun, Y.-L.; Huang, W.-J.; Lee, S.-H. Formation of Octatetrayne (HC_8H) from the Reaction of Butadiynyl (C_4H) with Butadiyne (HC4H). *Chem. Phys. Lett.* **2017**, *690*, 147−152.
(28) Landera, A.; Krishtal, S. P.; Kislov, V. V.; Mebel, A. M.; Kaiser, R. I. Theoretical Study of the C_6H_3 Potential Energy Surface and Rate Constants and Product Branching Ratios of the C_2H-($^2\sum^+$)+C_4H_2($^1\sum_g^+$) and C_4H($^2\sum^+$)+C_2H_2($^1\sum_{g+}$) Reactions. *J. Chem. Phys.* **2008**, *128* (21), No. 214301.
(29) Kaiser, R. I.; Stahl, F.; Schleyer, P. V. R.; Schaefer, H. F., III Atomic and Molecular Hydrogen Elimination in the Crossed Beam Reaction of D1-Ethinyl Radicals C_2D($X\ ^2\sum^+$) with Acetylene, C_2H_2($X\ ^1\sum_g^+$): Dynamics of D1-Diacetylene (HCCCCD) and D1-Butadiynyl (DCCCC) formationPresented at the XIX International Symposium on Molecular Beams, Rome, 3−8 June, 2001. *Phys. Chem. Chem. Phys.* **2002**, *4* (13), 2950−2958.
(30) Gu, X.; Kim, Y. S.; Kaiser, R.; Mebel, A. M.; Liang, M.; Yung, Y. Chemical Dynamics of Triacetylene Formation and Implications to the Synthesis of Polyynes in Titan's Atmosphere. *Proc. Natl. Acad. Sci. U.S.A.* **2009**, *106*, 16078−16083.
(31) Jones, B. M.; Zhang, F.; Kaiser, R. I.; Jamal, A.; Mebel, A. M.; Cordiner, M. A.; Charnley, S. B. Formation of Benzene in the Interstellar Medium. *Proc. Natl. Acad. Sci. U.S.A.* **2011**, *108* (2), 452−457.
(32) Dangi, B. B.; Parker, D. S. N.; Kaiser, R. I.; Jamal, A.; Mebel, A. M. A Combined Experimental and Theoretical Study on the Gas-Phase Synthesis of Toluene under Single Collision Conditions. *Angew. Chem., Int. Ed.* **2013**, *52* (28), 7186−7189.
(33) Thomas, A. M.; He, C.; Zhao, L.; Galimova, G. R.; Mebel, A. M.; Kaiser, R. I. Combined Experimental and Computational Study on the Reaction Dynamics of the 1-Propynyl (CH_3CC)−1,3-Butadiene ($CH_2CHCHCH_2$) System and the Formation of Toluene under Single Collision Conditions. *J. Phys. Chem. A* **2019**, *123* (19), 4104−4118.
(34) Glicker, S.; Okabe, H. Photochemistry of Diacetylene. *J. Phys. Chem.* **1987**, *91* (2), 437−440.
(35) Kaiser, R. I.; Parker, D. S. N.; Mebel, A. M. Reaction Dynamics in Astrochemistry: Low-Temperature Pathways to Polycyclic Aromatic Hydrocarbons in the Interstellar Medium. *Annu. Rev. Phys. Chem.* **2015**, *66* (1), 43−67.
(36) Lee, Y. T. Molecular Beam Studies of Elementary Chemical Processes. *Science* **1987**, *236* (4803), 793−798.
(37) Herschbach, D. R. Molecular Dynamics of Elementary Chemical Reactions (Nobel Lecture). *Angew. Chem., Int. Ed. Engl.* **1987**, *26* (12), 1221−1243.
(38) Berteloite, C.; Le Picard, S. D.; Balucani, N.; Canosa, A.; Sims, I. R. Low Temperature Rate Coefficients for Reactions of the Butadiynyl Radical, C 4 H, with Various Hydrocarbons. Part I: Reactions with Alkanes (CH 4, C 2 H 6, C 3 H 8, C 4 H 10). *Phys. Chem. Chem. Phys.* **2010**, *12* (15), 3666−3676.

https://doi.org/10.1021/acs.jpclett.4c03150
J. Phys. Chem. Lett. 2025, 16, 658−666

(39) Berteloite, C.; Le Picard, S. D.; Birza, P.; Gazeau, M.-C.; Canosa, A.; Bénilan, Y.; Sims, I. R. Low Temperature (39−298 K) Kinetics Study of the Reactions of the C4H Radical with Various Hydrocarbons Observed in Titan's Atmosphere. *Icarus* **2008**, *194* (2), 746−757.
(40) Berteloite, C.; Le Picard, S. D.; Balucani, N.; Canosa, A.; Sims, I. R. Low Temperature Rate Coefficients for Reactions of the Butadiynyl Radical, C 4 H, with Various Hydrocarbons. Part II: Reactions with Alkenes (Ethylene, Propene, 1-Butene), Dienes (Allene, 1,3-Butadiene) and Alkynes (Acetylene, Propyne and 1-Butyne). *Phys. Chem. Chem. Phys.* **2010**, *12* (15), 3677−3689.
(41) Zhou, L.; Kaiser, R. I.; Tokunaga, A. T. Infrared Spectroscopy of Crystalline and Amorphous Diacetylene (C_4H_2) and Implications for Titan's Atmospheric Composition. *Planetary and Space Science* **2009**, *57* (7), 830−835.
(42) Jones, A. V.; Herzberg, G. Infra-Red and Raman Spectra of Diacetylene. *Proceedings of the Royal Society of London. Series A. Mathematical and Physical Sciences* **1997**, *211* (1105), 285−295.
(43) Okabe, H. Photochemistry of Acetylene at 1470 Å. *J. Chem. Phys.* **1981**, *75* (6), 2772−2778.
(44) Proch, D.; Trickl, T. A High-intensity Multi-purpose Piezoelectric Pulsed Molecular Beam Source. *Rev. Sci. Instrum.* **1989**, *60* (4), 713−716.
(45) Chai, J.-D.; Head-Gordon, M. Long-Range Corrected Hybrid Density Functionals with Damped Atom−Atom Dispersion Corrections. *Phys. Chem. Chem. Phys.* **2008**, *10* (44), 6615−6620.
(46) Becke, A. D. Density-Functional Thermochemistry. III. The Role of Exact Exchange. *J. Chem. Phys.* **1993**, *98* (7), 5648−5652.
(47) Lee, C.; Yang, W.; Parr, R. G. Development of the Colle-Salvetti Correlation-Energy Formula into a Functional of the Electron Density. *Phys. Rev. B* **1988**, *37* (2), 785−789.
(48) Adler, T. B.; Knizia, G.; Werner, H.-J. A Simple and Efficient CCSD(T)-F12 Approximation. *J. Chem. Phys.* **2007**, *127* (22), No. 221106.
(49) Knizia, G.; Adler, T. B.; Werner, H.-J. Simplified CCSD(T)-F12 Methods: Theory and Benchmarks. *J. Chem. Phys.* **2009**, *130* (5), No. 054104.
(50) Dunning, T. H., Jr. Gaussian Basis Sets for Use in Correlated Molecular Calculations. I. The Atoms Boron through Neon and Hydrogen. *J. Chem. Phys.* **1989**, *90* (2), 1007−1023.
(51) Curtiss, L. A.; Raghavachari, K.; Redfern, P. C.; Rassolov, V.; Pople, J. A. Gaussian-3 (G3) Theory for Molecules Containing First and Second-Row Atoms. *J. Chem. Phys.* **1998**, *109* (18), 7764−7776.
(52) Curtiss, L. A.; Raghavachari, K.; Redfern, P. C.; Baboul, A. G.; Pople, J. A. Gaussian-3 Theory Using Coupled Cluster Energies. *Chem. Phys. Lett.* **1999**, *314* (1−2), 101−107.
(53) Baboul, A. G.; Curtiss, L. A.; Redfern, P. C.; Raghavachari, K. Gaussian-3 Theory Using Density Functional Geometries and Zero-Point Energies. *J. Chem. Phys.* **1999**, *110* (16), 7650−7657.
(54) Zhang, J.; Valeev, E. F. Prediction of Reaction Barriers and Thermochemical Properties with Explicitly Correlated Coupled-Cluster Methods: A Basis Set Assessment. *J. Chem. Theory Comput.* **2012**, *8* (9), 3175−3186.
(55) Frisch, M. J.; Trucks, G. W.; Schlegel, H. B.; Scuseria, G. E.; Robb, M. A.; Cheeseman, J. R.; Scalmani, G.; Barone, V.; Mennucci, B.; Petersson, G. A.; Nakatsuji, H.; Caricato, M.; Li, X.; Hratchian, H. P.; Izmaylov, A. F.; Bloino, J.; Zheng, G.; Sonnenberg, J. L.; Hada, M.; Ehara, M.; Toyota, K.; Fukuda, R.; Hasegawa, J.; Ishida, M.; Nakajima, T.; Honda, Y.; Kitao, O.; Nakai, H.; Vreven, T.; Montgomery, J. A.; Peralta, J. E.; Ogliaro, F.; Bearpark, M.; Heyd, J. J.; Brothers, E.; Kudin, K. N.; Staroverov, V. N.; Kobayashi, R.; Normand, J.; Raghavachari, K.; Rendell, A.; Burant, J. C.; Iyengar, S. S.; Tomasi, J.; Cossi, M.; Rega, N.; Millam, J. M.; Klene, M.; Knox, J. E.; Cross, J. B.; Bakken, V.; Adamo, C.; Jaramillo, J.; Gomperts, R.; Stratmann, R. E.; Yazyev, O.; Austin, A. J.; Cammi, R.; Pomelli, C.; Ochterski, J. W.; Martin, R. L.; Morokuma, K.; Zakrzewski, V. G.; Voth, G. A.; Salvador, P.; Dannenberg, J. J.; Dapprich, S.; Daniels, A. D.; Farkas, Ö.; Foresman, J. B.; Ortiz, J. V.; Cioslowski, J.; Fox, D. J. *Gaussian 09*, Revision A.1; Gaussian Inc., Wallingford, CT, 2009.
(56) Werner, H.-J.; Knowles, P. J.; Lindh, R.; Manby, F. R.; Schütz, M.; Celani, P.; Korona, T.; Rauhut, G.; Amos, R. D.; Bernhardsson, A. *MOLPRO, Revision 2015.1, A Package of Ab Initio Programs*; University of Cardiff, Cardiff, UK, 2015.
(57) Steinfeld, J. I.; Francisco, J. S.; Hase, W. L. *Chemical Kinetics and Dynamics*, 2nd ed..; Pearson: Upper Saddle River, NJ, 1998.
(58) Eyring, H.; Lin, S. H.; Lin, S. M. *Basic Chemical Kinetics*; John Wiley and Sons: New York, 1980.
(59) Robinson, P. J.; Holbrook, K. A. *Unimolecular Reactions*; John Wiley and Sons: New York, 1972.
(60) He, C.; Zhao, L.; Thomas, A. M.; Morozov, A. N.; Mebel, A. M.; Kaiser, R. I. Elucidating the Chemical Dynamics of the Elementary Reactions of the 1-Propynyl Radical (CH_3CC; X^2A_1) with Methylacetylene (H_3CCCH; X^1A_1) and Allene (H_2CCCH_2; X^1A_1). *J. Phys. Chem. A* **2019**, *123* (26), 5446−5462.
(61) Kislov, V. V.; Nguyen, T. L.; Mebel, A. M.; Lin, S. H.; Smith, S. C. Photodissociation of Benzene under Collision-Free Conditions: An Ab Initio/Rice−Ramsperger−Kassel−Marcus Study. *J. Chem. Phys.* **2004**, *120* (15), 7008−7017.

https://doi.org/10.1021/acs.jpclett.4c03150
J. Phys. Chem. Lett. 2025, 16, 658−666